Current Trends in Biotechnology and Pharmacy
Vol. 17(Supplementary issue - 3B) 1271-1277,September 2023, ISSN 0973-8916 (Print), 2230-7303 (Online)
10.5530/ctbp.2023.3s.62

Fluoroscopic Imaging Automation through Linear Regression and Diagnosing through Convolutional Neural Networks

Karthi M*, Raghul G, Priscilla R

Department of Information Technology, St. Joseph's Institute of Technology, Chennai
*Corresponding author: mmuthukarthi@gmail.com

Abstract

Fluoroscopic imaging is a medical and pharmaceutical biotechnology imaging process that uses x-rays to capture moving pictures of the internal parts and organs of the body. These images can aid in the detection of fractures and other types of bodily injury. Dosage Area Product (DAP) (also known as Kerma Area Product (KAP)) is an important statistic used to quantify the level of radiation dose for each organ. It is determined by multiplying the absorbed dosage by the area of the x-ray field. The standard approach for determining the primary components in fluoroscopic pictures is challenging due to the high possibility of error rates. This paper proposes an automated approach for fluoroscopic imaging using Linear Regression and Convolutional Neural Networks (CNN). This approach aims to improve the accuracy and reliability of identifying primary components in fluoroscopic images.

Keywords: Fluoroscopic Imaging, Dosage Area Product (DAP), Kerma Area Product (KAP), Automated Scope, Linear Regression, Convolutional Neural Networks (CNN)

Introduction

Medical imaging has advanced significantly in its ability to identify and treat various illnesses in both children and adults. Medical imaging comes in many forms, including computer tomography, fluoroscopy, radiography, mammography, and other procedures. Fluoroscopic imaging is a medical imaging technique that employs a monitor to display continuous x-ray images, similar to an X-ray. During fluoroscopic imaging, an X-ray beam is passed through the body, and the resulting image is sent to a display where the movement of a body part, instrument, or contrast agent such as an X-ray beam can be observed. The imaging team is responsible for maintaining and delivering the proper radiation dosage. An interesting fact is that the FDA oversees manufacturers of fluoroscopic x-ray equipment under the EPRC (Electronic Product Radiation Control) and Medical division sections of the Federal Food, Drug, and Cosmetic Act. Section II of this paper discusses various methods for estimating skin dosage, while Section III explores Dose Area Product, one of the most promising approaches in fluoroscopic imaging.

Dose area product

Dosimetric information plays a crucial role in medical imaging. It is important to ensure that all techniques for assessing skin dosage pass physical and quality assurance tests. These techniques help maintain dose rate limitations on clinical equipment. One study [1] outlines several methods for assessing skin dose

Vol. 17(Supplementary issue - 3B) 1271-1277,September 2023, ISSN 0973-8916 (Print), 2230-7303 (Online)
10.5530/ctbp.2023.3s.62

for medical imaging, including indirect real-time dose monitoring, which calculates a dose at a specific location using a physical measurement at a convenient point or based on equipment operating characteristics and system geometry.

In interventional fluoroscopy laboratories, the fluoroscopic timer is often used as the sole dose measure, which can result in inadequate skin dose calculations due to various factors. However, the use of Dose Area Product (DAP) has increased in recent years due to its ease of computation and good correlation with the total energy to effective dose conveyed to the patient. In a study [2] involving 421 adult patients who underwent conventional radiography exams, the mean effective dose was estimated using Exposure Area Product (EAP), Air Kerma, and Entrance Surface Doses (ESD). However, DAP was used to match the precise quantity. The mean effective doses for chest, abdomen, cervical spine, lumbar spine, pelvis, and skull examinations were found to be 0.13, 0.42, 0.05, 0.59, 0.54, and 0.03 mSv/projection, respectively.

Proposed work

Finding the dose area product of the particular organ

Machine learning refers to the use and advancement of intelligent computer systems that can learn and adapt to solve a given problem or perform a particular task using different algorithms and statistical models. The medical industry has found machine learning to be valuable because of its ability to make complex logical decisions without human intervention. Over the years, machine learning has been employed to create more accurate diagnostic tools for analyzing medical images, identifying the underlying cause, and diagnosing patients for their illnesses using deep learning techniques that replicate the decision-making capabilities of the human brain.

Linear regression [3] predicts the dependent variable value (y) based on the independent variable (x). The dependent variable is the one you want to forecast, and the independent variable is the one you're using to predict the value of the other variable. The 'line of best fit' is the plotting of two sets of data points against one another. A linear combination of the input variables is the simplest basic linear regression model.

$$- \ y(x,w) \ = \ w0 \ + \ w1x1 + \ldots + wDxD \ - \quad (1)$$

where $x = (x1,\ldots,xD)$ This is commonly referred to as linear regression. This model's main feature is that it is a linear function of the $w0,\ldots,wD$. parameters. It is, however, a linear function of the input variables xi, which limits the model significantly.

Batch techniques that entail processing the entire training set in one go may be computationally costly for large data sets. Sequential algorithms, often known as on-line algorithms, may be beneficial if the data set is large enough. In which data points are considered one at a time, and model parameters are changed after each such presentation. Sequential learning is especially appropriate for real-time applications when data observations occur in a continuous stream and predictions must be established prior to viewing all data points [4].

Diagnosing the images through convolutional neural networks

CNN, or Convolutional Neural Network [5], is an Artificial Neural Network (ANN) model that improves performance by working on image, speech, and audio signal inputs. All ANNs, as we know, have performance layers to some extent; the three basic layers are the convolution layer, the pooling layer, and the fully-connected layer.

A CNN's first layer is the convolution layer. It is followed by a slew of additional convolution layers or the pooling layer. The fundamental characteristics are provided by the convolution layer, which handles the majority of the effort. Input data, a filter, and a feature map are the essential components. In this scenario, the input data is an image with three distinct dimensions; the filter or kernel will run across the image to identify the presence of the characteristic; this is referred to as the feature detector. The feature

Vol. 17(Supplementary issue - 3B) 1271-1277,September 2023, ISSN 0973-8916 (Print), 2230-7303 (Online)
10.5530/ctbp.2023.3s.62

detector is a collection of weights that represent a section of an image. They can be both a 2-D array and a 3-by-3 matrix that determines the size of each field since they are incorrectly proportioned.

When the filter is applied to a picture, a dot product between the filter and the input pixels is formed, which is then applied to the output array. This step is repeated until the filter completely covers the target picture in hand. The output of the filters' dot products is known as feature maps or convoluted features. To be more specific, the convolutional layer turns the picture into numerical values, creating important patterns to aid in data interpretation.

The pooling layer (down sampling) performs discretization to reduce the number of parameters in the incoming data. The pooling technique works by evaluating the overall input as well as the suitability of the image input. This filter has no weight; instead, it executes an aggregation function on the field values, filling the output array. Pooling may be classified into two types:

Max pooling: The process of selecting the pixel with the highest value to send to the output array.

Pooling on average: It is the process of choosing the average values from each field to deliver to the output array. Each node in the output layer is directly connected to the nodes in the preceding layer in this layer. It classifies the information based on the characteristics retrieved by the preceding layers and kernels, producing a probability of 0 to 1 in the process.

Afshar et al. [6] developed a capsule network-based framework model for diagnosing Covid-19 (i.e., COVIDCAAPS) sickness using X-ray images. Convolution layers and capsules are employed in this suggested effort to address the issue of class imbalance. In an experimental study, they demonstrated COVIDCAPS's high performance on fewer trainable parameters. Alqudah et al. [7] recommended a hybrid artificially intelligent system that combines deep learning and machine learning techniques, namely convolutional neural network (CNNs) and softmax classifiers. The proposed approach was created specifically to diagnose Covid-19 patients using chest X-ray images. Choi et al. [8] suggest a diagnostic imaging study of a novel coronavirus in the Middle East Respiratory Syndrome (MERS). They looked at the case of a 30-year-old male patient who had diarrhoea, fever, and stomach pain. The authors looked at the use of chest X-rays in the treatment of sick people [9]. They also used this model on a collection of chest X-ray and CT pictures and got better results. Furthermore, Basile et al. [10] addressed what processes hospital professionals must follow in order to reduce the risk to healthy individuals, in addition to the precautionary measures that must be used when caring for covid-19 disease patients.

Overall architecture

The table 1 describes the effective mean doses, specifically for various organs of the body.

Table 1**.** Effective Mean Doses taken for 421 patients based on gender, projection, and Organs

Name of the Organ	Gender	Projection	Mean Effective Dose
Chest	Male	PA	0.123
Chest	Transgender	PA	0.122
Chest	Female	PA	0.121
Chest	Male	AP	0.123
Chest	Transgender	AP	0.122
Chest	Female	AP	0.121
Abdomen	Male	AP	0.381
Abdomen	Transgender	AP	0.42
Abdomen	Female	AP	0.46
Skull	Male	PA	0.381
Skull	Transgender	PA	0.381
Skull	Female	PA	0.381
Pelvis	Male		0.472
Pelvis	Transgender		0.521
Pelvis	Female		0.607
Cervical Spine	Male		0.082
Cervical Spine	Transgender		0.08

Vol. 17(Supplementary issue - 3B) 1271-1277,September 2023, ISSN 0973-8916 (Print), 2230-7303 (Online)
10.5530/ctbp.2023.3s.62

Cervical Spine	Female		0.079
Lumbar Spine	Male		0.566
Lumbar Spine	Female		0.981
Lumbar Spine	Transgender		0.722

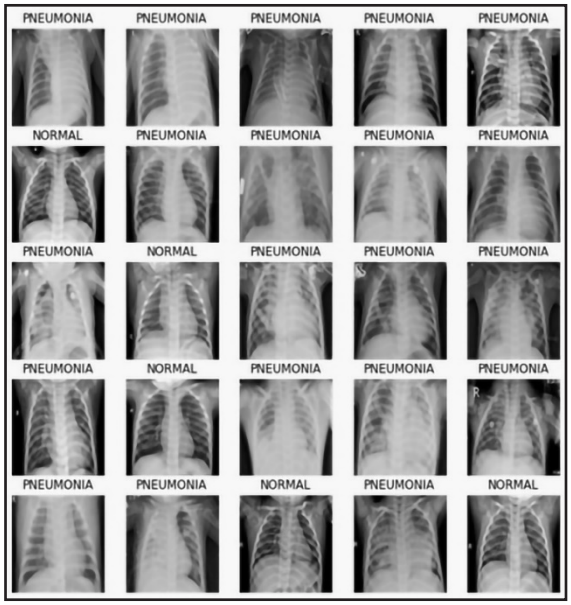

Fig. 1. Sample images of two different classes namely Normal and Pneumonia

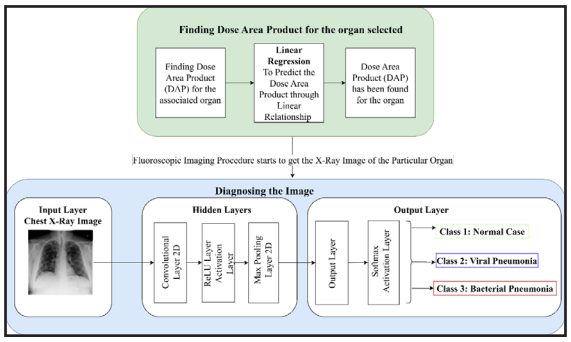

Fig. 2. Overall Architecture Diagram

The image is sent as an input to CNN, which uses two convolutional layers and two maximum pooling layers to analyze the image and determine three classes of outputs: bacterial pneumonia, viral pneumonia, and Normal Case. Figure 1 depicts the example classes of photos used for categorization. The output layer's Softmax Activation layer is used to categorize the picture based on the probability distribution. Linear regression is used to predict the Dose Area Product (DAP) of a particular organ. After finding the Dose Area Product (DAP), the fluoroscopic imaging process is carried out, the image is diagnosed through Convolutional Neural Networks (CNN) to classify the images based on training samples. The overall architecture of the proposed work is depicted in fig. 2.

Results and Discussion

The evaluation metrics calculated are Mean Absolute Error (MAE), Mean Squared Error (MSE), Mean Absolute Percentage Error (MAPE), Mean Relative Error (MRE), Root Mean Squared Error (RMSE), and R2 Score respectively. Equation 2, 3, 4, 5, 6, and 7 represents the evaluation metrics equation used to evaluate the linear regression model used, where y_i is the predicted measure, x_i is the true value, n is the total number of data points, is the predicted values, At is the actual value, Ft is the forecast value, N is the number of non-missing data points, RSS is the sum of squares of residuals, TSS is the total sum of squares respectively.

$$MAE = \sum_{i=1}^{n} \frac{|yi - xi|}{n} - (2)$$

$$MSE = \frac{1}{n}\sum_{i=1}^{n}\left(Yi - \hat{Y}\imath\right)^2 - (3)$$

$$MPSE = \frac{1}{n}\sum_{t=1}^{n}\left|\frac{At - Ft}{At}\right| - (4)$$

$$MRE = \left(\frac{AbsoluteError}{Truevalue}\right) * 100\% - (5)$$

$$RMSE = \sqrt{\sum_{i=1}^{N}\frac{(x^i - \hat{x})^2}{N}} - (6)$$

$$R^2 = 1 - \left(\frac{RSS}{TSS}\right) - (7)$$

Vol. 17(Supplementary issue - 3B) 1271-1277,September 2023, ISSN 0973-8916 (Print), 2230-7303 (Online)
10.5530/ctbp.2023.3s.62

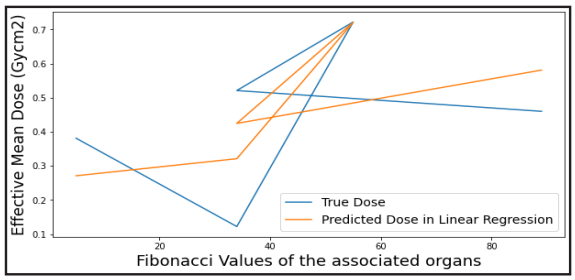

Fig. 3. Actual vs Predicted Value graph of DAP using Linear Regression

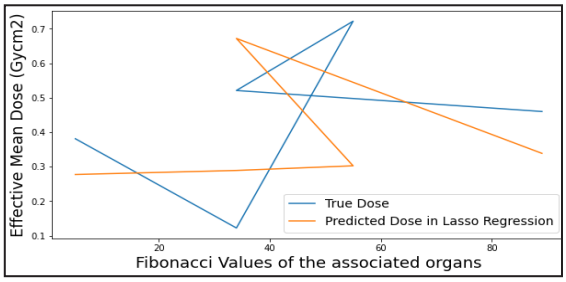

Fig. 4. Actual vs Predicted Value graph of DAP using Lasso Regression

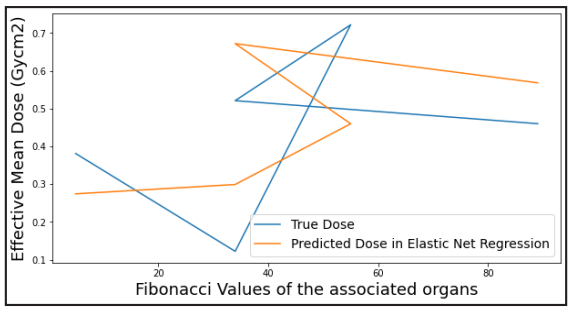

Fig. 5. Actual vs Predicted Value graph of DAP using Elastic Net Regression

As research, we took Lasso Regression, and Elastic Net Regression, and Linear Regression to test the efficiency of the model. But Linear Regression stands first in predicting the dose area product at the correct scale to provide a better regression score. Fig. 3, 4, and 5 shows Actual vs Predicted Value graph of Dose Area Product (DAP) using Linear Regression, Lasso Regression, and Elastic Net Regression respectively. In the figures, x axis gives the associated Fibonacci value of the organ and y axis gives the effective mean doses. As the graph shows, Linear Regression behaves as same as the actual mean dose given in the database taken. This clearly shows evidence that Linear Regression behaves well than the other models taken in this research.

Table 2 gives the evaluation metrics of all the regression models used in this research. Fig. 6, 7 and 8 gives the Error Variation stem plots from all the regression models used in this research to diagnose the errors detected in predicting the dose area product. In the figures, x axis gives the Fibonacci Values of the associated organs and y axis gives the Variation in True Effective Mean Dose and Effective Mean Dose, measured in ($Gycm^2$). From the figures, Error Stem plot in Linear Regression doesn't stand up more than 0.10 in difference. After finding the dose area product, fluoroscopic imaging starts. The image is then diagnosed through the CNN algorithm. The CNN is constructed by three different layers as hidden layers. The training dataset has two different features namely Normal and Pneumonia. The Accuracy graph and the Model's Loss graph are given in fig. 9 respectively.

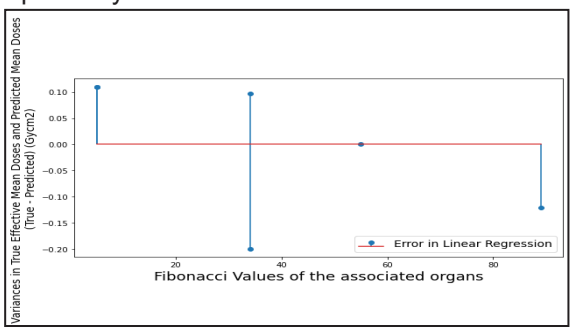

Fig. 6. Error Variation in DAP in Linear Regression

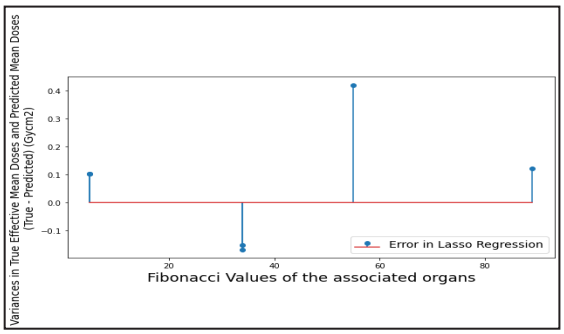

Fig. 7. Error Variation in DAP in Lasso Regression

Vol. 17(Supplementary issue - 3B) 1271-1277,September 2023, ISSN 0973-8916 (Print), 2230-7303 (Online)
10.5530/ctbp.2023.3s.62

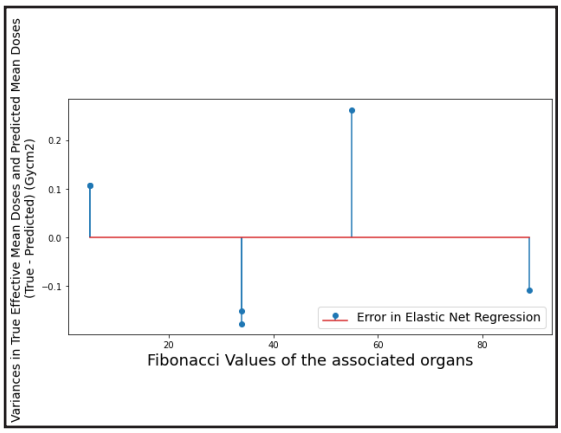

Fig. 8. Error Variation in DAP in Elastic Net Regression

Table 2. Evaluation Metrics of all Regression Models used

Evaluation Metrics	Linear	Lasso	Elastic-Net
Mean Absolute Error (MAE)	0.164	0.775	0.687
Mean Squared Error (MSE)	0.040	0.050	0.046
Mean Absolute Percentage Error (MAPE)	0.415	0.624	0.654
Mean Relative Error (MRE)	0.415	0.625	0.638
Root Mean Squared Error (RMSE)	0.200	0.210	0.217
R2 Score	0.756	0.560	0.656

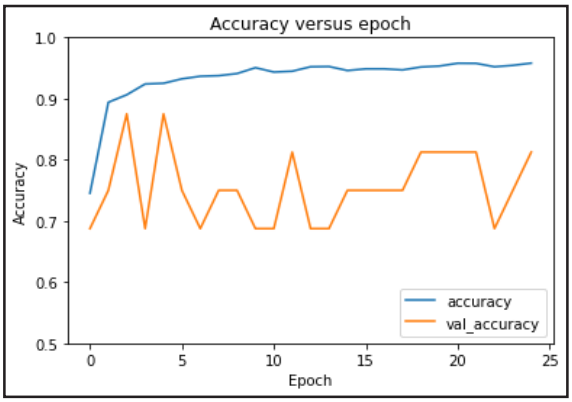

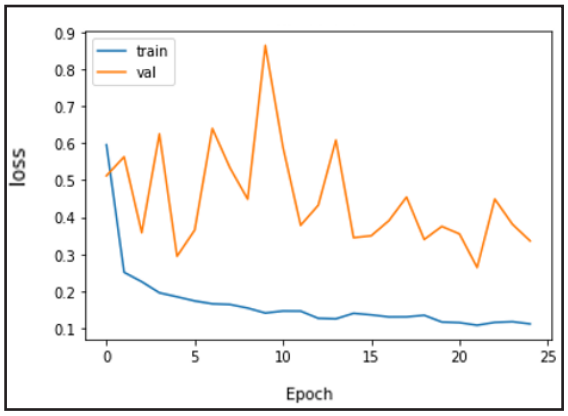

Fig. 9. Accuracy vs epoch and loss graph of CNN Model used in Multi Class Classification

Conclusion & Future Approach

Medical imaging plays a crucial role in diagnosing illnesses in both newborns and adults, including fractures, pneumonia, and more recently, Covid-19. With the continuous expansion and development of medical imaging technology, each method has shown its competence in detecting dangerous and curable disorders. Fluoroscopy imaging, in particular, uses a monitor to display continuous X-ray images, similar to an X-ray, by injecting an X-ray beam into the body and capturing the mobility of a body part, device, or contrasting agent. Artificial intelligence (AI) has been introduced to simplify the procedure by providing adequate resources to the model to appropriately diagnose the image's nature (11). The Quantum Teleportation Protocol, as employed in DICOM (Digital Imaging and Communication), ensures the safe transmission of fluoroscopic pictures and data to a centralized database.

The next step in the study is to optimize the model for all types of fluoroscopic imaging to identify conditions on a wider scale. This can be achieved by enhancing the model's understanding of various illnesses and making it quicker and more efficient in identifying them. The future of medical imaging depends on technical advancements that enhance cell-level visibility and computation speed. The use of AI and

Vol. 17(Supplementary issue - 3B) 1271-1277,September 2023, ISSN 0973-8916 (Print), 2230-7303 (Online)
10.5530/ctbp.2023.3s.62

machine learning (ML) as diagnostic and interpretation tools for medical images will become increasingly common (12).

References

1. Balter, S. (2006) Methods for measuring fluoroscopic skin dose. Pediatr Radiol, 36(2), 136-140.

2. Bahreyni, T. S., Nazeri, M., & Zare, H. (2006) Application of dose-area product compared with three other dosimetric quantities used to estimate patient effective dose in diagnostic radiology, J Radiat Res, 4(1), 21-27.

3. Seber, G. A., & Lee, A. J. (2003) Linear regression analysis (Vol. 330). John Wiley & Sons.

4. Gladence, L. M., Karthi, M., & Anu, V. M. (2015) A statistical comparison of logistic regression and different Bayes classification methods for machine learning. ARPN J Engg Appd Sci, 10(14), 5947-5953.

5. Roska, T., & Chua, L. O. (1993) The CNN paradigm. IEEE Trans. Circuits Syst. I Fundam. Theory Appl, 40(3), 147-156.

6. Afshar, P., Heidarian, S., Naderkhani, F., Oikonomou, A., Plataniotis, K. N., & Mohammadi, A. (2020) Covid-caps: A capsule network-based framework for identification of covid-19 cases from x-ray images. Pattern Recognit Lett, 138, 638-643.

7. Alqudah, A. M., Qazan, S., & Alqudah, A. (2020) Automated systems for detection of COVID-19 using chest X-ray images and lightweight convolutional neural networks. Emerg Radiol, 4(1), 54-67.

8. Choi, W. J., Lee, K. N., Kang, E. J., & Lee, H. (2016) Middle East respiratory syndrome-coronavirus infection: a case report of serial computed tomographic findings in a young male patient. Korean J Radiol, 17(1), 166-170.

9. Ayan, E., & Ünver, H. M. (2019) Diagnosis of pneumonia from chest X-ray images using deep learning. Sci Meet Electr Biomed Eng Comput Sci EBBT, 1-5.

10. Basile, C., Combe, C., Pizzarelli, F. (2020) Recommendations for the prevention, mitigation and containment of the emerging SARS-CoV-2 (COVID-19) pandemic in haemodialysis centres. Nephrol Dial Transplant, 35(5), 737-741.

11. Sharma, N., Gupta, S., Gupta, M., & Chandra, S. (2021) Transfer Learning-Based Attention Gated Siamese Network for Human and SARS-CoV-2 Protein Interactions. Curr Trends Biotechnol Pharm, 15(6), 80-82.

12. Oguri, V. S. B., & Poda, S. (2022) Automated Detection of Breast Cancer Using Machine Learning Algorithms: A Comparative Analysis. Curr Trends Biotechnol Pharm, 16(4): 481-489.